第 48 卷 第 10 期
2021 年 10 月

湖南大学学报（自然科学版）
Journal of Hunan University（Natural Sciences）

Vol. 48 No. 10
October 2021

Open Access Article

Comparative FTIR Study of Treated Hemp Hurds before and after Their Application in Bio-Aggregate-Based Composites

Nadezda Stevulova[1*], Eva Singovszka[1], Stefan Demcak[2]

[1] Institute of Environmental Engineering, Faculty of Civil Engineering, Technical University of Kosice, Vysokoskolska 4, 042 00 Kosice, Slovakia

[2] Department of Environmental Management, Faculty of Management, University of Presov, Ul. Konštantínova 16, 080 01 Prešov, Slovakia

Abstract: The incorporation of bio-aggregates in composites with inorganic matrix has become popular nowadays. This paper aims to investigate the effect of alternative binder (MgO-cement) on the degradation of reference and treated hemp hurds bio-aggregates during their long-term incorporation in the composites. Changes in the molecular structures and associated chemical bonds of the chemically (sodium hydroxide NaOH, calcium hydroxide $Ca(OH)_2$, and ethylenediaminetetraacetic acid (EDTA)) and physicochemical (ultrasound in water and NaOH solution) modified and long-term embedded hemp hurds bio-aggregates in composite compared to reference hemp slices using Fourier-transform infrared (FTIR) spectroscopy as one of the most popular methods for testing lignocellulosic materials were studied. The spectra of reference and ultrasound treated bio-aggregates, used for Portland cement matrix reinforcing, were also reported for comparison. The degree of cellulose crystallinity was used to assess the degradation of hemp hurds samples after treatment and their application in the composite. FTIR spectra have shown some similarity in bands positions representing the main hemp hurds components and binder hydrated phases (magnesium silicate hydrate M-S-H and calcium silicate hydrate C-S-H, respectively). However, the spectra revealed changes in cellulose crystallinity depending on the behavior of the surface-modified hemp hurds structure during their long-term interaction with binder particles in the composite. The evaluation of bio-aggregate samples' performance due to their long-term incorporation in composite matrix confirmed an effect of the alkaline environment of binders on cellulose crystallinity.

Keywords: hemp hurd, treatment, bio-aggregate-based composite, Fourier-transform infrared spectroscopy, degree of cellulose crystallinity.

處理過的大麻塊在生物集料基複合材料中應用前後的傅里葉變換紅外比較研究

摘要：將生物聚集體摻入具有無機基質的複合材料中已成為當今的流行趨勢。本文旨在研究替代粘合劑（氧化鎂-
水泥）在長期摻入複合材料期間對參考和處理過的大麻纖維生物聚集體降解的影響。化學（氫氧化鈉氫氧化鈉、氫氧化鈣氫氧化鈣
和乙二胺四乙酸）和物理化學（水和氫氧化鈉溶液中的超聲）改性和長期嵌入的大麻障礙生物聚集體的分子結構和相關化學鍵的變化使用傅立葉變換紅外光譜作為測試木質纖維素材料的最流行方法之一，將復合材料與參考大麻切片進行比較。還報告了用於波特蘭水泥基體增強的參考和超聲處理生物集料的光譜以進行比較。纖維素結晶度用於評估處理後大麻障礙樣品的降解及其在復合材料中的應用。傅里葉變換紅外光譜在代表主要大麻障礙組分和粘合劑的水合相（分別是水合矽酸鎂和水合矽酸鈣）的波段位置顯示出一些相似性。然而，光譜顯示纖維素結晶度的變化取決於表面改性的大麻障礙結構在與復合材料中的粘合劑顆粒長期相互作用期間的行為。由於生物聚集體樣品長期摻入複合基質中而對其性能的評估證實了粘合劑的鹼性環境對纖維素結晶度的影響。

Received: June 7, 2021 / Revised: August 3, 2021 / Accepted: September 1, 2021 / Published: October 30, 2021

Fund Project: National Natural Science Foundation of China (00000000), National Natural Science Foundation of China (00000000)

About the authors: Nadezda Stevulova, Eva Singovszka, Institute of Environmental Engineering, Faculty of Civil Engineering, Technical University of Kosice, Kosice, Slovakia; Stefan Demcak, Department of Environmental Management, Faculty of Management, University of Presov, Prešov, Slovakia

Corresponding author Nadezda Stevulova, nadezda.singovszka@tuke.sk

关键词：大麻赫德，處理，基於生物聚集體的複合材料，傅里叶变换红外光谱，纖維素結晶度。

1. Introduction

The increasing global energy consumption, economic crisis, and environmental risks have encouraged research to exploit renewable raw materials to produce environmentally friendly materials. Recently, the hotspot interest in rapidly renewable raw materials resources such as plant fibers with high tensile strength as a good reinforcing component and/or organic filler into lightweight bio-composite materials is recorded. The automobile and construction industries [1-3] are the key sectors employing bio-composites. The potential of bio-composites to be used as eco-friendly, renewable, and sustainable is the main driving force for research, development, and commercialization. They are promising materials providing an overcoming of high environmental impacts of the construction and building sectors that are mainly related to the high consumption of raw materials, energy demand (40% of all energy), and significant contribution to greenhouse emissions (36% of all CO_2 emissions). Therefore the development of bio-composites for the construction sector could play a key role in transitioning an oil-based economy towards a bio-based economy [4]. Many investigations aimed to utilize biomass lignocellulosic materials in the form of natural fibers and /or waste fibrous bio-aggregates into sustainable bio-composite products [5, 6]. The increasing use of plant lignocellulosic resources into composites with the inorganic matrix is due to their good mechanical properties, biodegradability, non-toxicity, and low carbon footprint [7, 8]. These specific properties make lignocellulosic material an attractive alternative filler component in bio-aggregate-based concretes [9].

Many studies focused on developing new building bio-based materials have a character linking interdisciplinary and sustainability in research to increase the sustainability level of the building industry [10, 11]. At present, hemp as a source of plant raw material is considered industrially and economically important not only for the production of building materials but also for paper, textiles, food, medicine, paints, detergents, varnishes, oils, and fuels too [12]. Industrial hemp (*Cannabis sativa L.*) is one of the world's oldest cultivated and fastest-growing annual fiber plants delivering fibers, hurds, and seeds. This crop is one the most available, has a very high yield of biomass with high cellulose content and unique properties (thermal, mechanical, acoustic, and aseptic). Due to these properties, environmental benefits, and low tetrahydrocannabinol (THC) content, hemp is considered a valuable vegetable plant for the bio-based economy [13]. Hemp hurds – waste from bast fibers processing, are used as lightweight bio-aggregate in the cementitious binder-bonded composite. However, the heterogeneity of bio-aggregates, presence of surface impurities, and a large number of hydroxyl groups lead to their high moisture sorption sensitivity, cause the chemical degradation of the structure, dimensional variations, which result in the development of a lower quality phase interface between lignocellulosic bio-aggregates and particles of the inorganic matrix in composite [14]. As known, the components of bio-aggregates embedded in composites undergo degradation leading to their decomposition in an alkaline environment justified by the low compatibility between hemp hurds and cementitious binder particles [15]. Dissolving the components of lignocellulosic materials (lignin and hemicellulose) in a cement pore solution and alkaline hydrolysis of cellulose molecules due to ongoing chemical reactions during the setting and hardening of composite significantly affect these processes at aggregate-binder interfacial zones, and it results in a weaker mechanical performance of the hardened bio-based composite. The mechanisms influencing the kinetics of binder hydration depend on the nature and quantity of the plant molecules extracted [16]. In order to eliminate the disadvantages of natural bio-aggregates and optimize their adhesive power with the matrix particles in composite, new approaches related to the substitution of conventional cement binder [17] and identifying a new way to treat hemp hurds have been applied [18]. Research of bio-based concrete with the most commonly used lime-based binders (e.g., hempcrete) has also been confirmed low compressive strength [19]. Better adhesive compatibility binder particles with hemp bio-aggregates compared to the lime-based binder were observed in bio-based composites with magnesia binders [20]. However, only a few studies were devoted to using magnesia cement in bio-based composites and evaluating their performance [21, 22]. The application of the surface-modified hemp hurds aggregates into composites enhanced mechanical properties in dependence on the binder nature. The long-term interactions between hemp bio-aggregate and MgO-cement involving complex processes are yet not fully understood. To the author's knowledge from the literature, no specific investigations of long-term incorporation of hemp hurds in composite with MgO-cement have been made.

However, the stability and durability of the produced bio-based composites after their long-term hardening are commonly verified from the point of view of the future use of the hemp hurds in commercial products but without studying changes in bio-aggregates.

Therefore, the scientific hypothesis of this work was focused on the elucidation of the causes of poorer compatibility hemp aggregates with particles MgO-cement in the interfacial zones of composite. The findings from our extensive research into the properties of original and modified hemp hurds [23, 24] and the technically important characteristics of the hardened bio-aggregate-based composites with MgO-cement [22, 25] supported it. The novelty of this paper is to give an insight explanation to the effect of MgO-cement matrix on the surface of chemically and physically modified hemp aggregates incorporated in the matrix and to understand the relationships between the qualitative changes of these composite components. This study was conducted on hemp hurds excluded from long-hardened composites with MgO-cement (calcined waste magnesite, silica sand, and alkaline compound, unlike the traditional composition of magnesia-based cement) highlights its significance and originality.

Following the conclusions of our published results, the aim of this work was focused on a comparative study of changes in the surface of the modified and long-term embedded hemp hurds aggregates in bio-based composite compared to reference bio-aggregate before and after its integration into a composite using FTIR spectroscopy. Also, the changes in cellulose crystallinity of hemp hurds samples affected by their long-term storage in composites with Portland cement and MgO-cement (observed by FTIR technique) were compared and discussed.

2. Materials and Methods

2.1. Original Hemp Hurds

This experimental study used bio-based aggregates of hemp hurds from the Netherlands Company Hempflax (Oude, Pekela) with a wide particle size distribution of particles (8-0.063 mm). Hemp hurds slices as a lightweight waste material (with the density of 117.5 kg/m^3) consisted of most hemp hurds over hemp bast fibers. It also contained fine dust particles as a residue from the processing of hemp stems, in particular from milling. Chemical analysis of a milled and oven-dried hemp hurds sample showed that the content of the cellulosic components was 77.28 wt% and non-cellulosic substances – 27.64 wt%, respectively.

2.2. Modified Hemp Hurds

Chemical treatment of hemp hurds was carried out in NaOH, $Ca(OH)_2$, and EDTA solution. Physico-chemical modification of hemp hurds was also made by its ultrasonication in water and 0.2 M NaOH solution. A more detailed characterization of the properties of modified hemp hurds has been described in [23, 24].

2.3. Modified Hemp Hurds

The long-term incorporated reference and modified hemp hurds slices (6 years) were excluded from the composite samples prepared from 40 vol. % of bio-aggregates, 29 vol. % of MgO-cement (consisting of the same portion of MgO, SiO_2, and $NaHCO_3$ components) and 31 vol. % of water. To better understand the impact of mineral binder on the bio-aggregate, two hemp hurds samples (reference and ultrasound treated) included in the Portland cement composites were used. The samples were subsequently dried at 60°C for 24 hours. The designation of the studied hemp hurd samples is given in Table 1.

Table 1 Nomenclature of the hemp hurd samples

Sample number	Hemp hurds sample	Designation
1	Reference (original)	H_{REF}
2	Reference (original) from AB matrix	H_{REF+AB}
3	Reference (original) from PC matrix	H_{ref+PC}
4	NaOH treated	H_{NaOH}
5	NaOH treated from AB matrix	$H_{NaOH+AB}$
6	$Ca(OH)_2$ treated	$H_{Ca(OH)2}$
7	$Ca(OH)_2$ treated from AB matrix	$H_{Ca(OH)2+AB}$
8	EDTA treated	H_{EDTA}
9	EDTA treated from AB matrix	$H_{EDTA+AB}$
10	Ultrasound treated in water	H_{USG}
11	Ultrasound treated in NaOH	$H_{USG+NaOH}$
12	Ultrasound treated from AB matrix	H_{USG+AB}
13	Ultrasound treated from PC matrix	H_{USG+PC}

2.4. Modified Hemp Hurds

After its treatment and subsequent long-term incorporation in the composite, the FTIR spectra of the original hemp hurds were obtained to characterize changes in the molecular structure and functional groups responsible for elements binding. The IR measurements were carried out on a Bruker Alpha Platinum-ATR spectrometer (BRUKER OPTICS, Ettingen, Germany). A total of 24 scans were performed on each sample, and the spectra were recorded in the range of 4,000-400 cm^{-1}.

In order to determine qualitative changes in cellulose crystallinity, ratios of two absorbance peaks at specific wave numbers were used [26]. The TCI value (the total crystallinity index) is based on the ratio of band intensities (1375/2900 cm^{-1}), and for lateral order index (LOI), this ratio was 1420/893 cm^{-1}. The band at around 1420-1430 cm^{-1} (assigned to asymmetric CH_2 bending vibration) is associated with the portion of the crystalline cellulose, while the band at around 890-898 cm^{-1} (assigned to a C-O-C stretching vibration at β-(1→4)-glycosidic linkages) is attributed

to the amorphous cellulose. The TCI is proportional to the crystallinity degree of cellulose, and LOI is correlated to the overall degree of ordering in cellulose. All the intensities of IR bands were normalized to the intensity of the 1024 cm^{-1} band in the deconvoluted spectra.

3. Results

3.1. Hemp Components

The complex structure of hemp hurds is primarily formed by cellulose, hemicelluloses, lignin, pectin, and waxes [18]. Hemp hurd (woody core) is one of the main parts of hemp stem, having lower cellulose content and higher lignin content than bast fibers [27]. Cellulose is the main component of hemp hurds (44.5%) is a linear polysaccharide polymer consisting of a molecular repeat unit comprised of a pair of d-anhydroglucose ring units joined by β-1→4 glycosidic oxygen linkages. Hemicellulose is the second important hemp component (32.8%) that is a heteropolymer (matrix polysaccharides) consisting of glucose and several other sugars (hexones, pentoses), uronic acids, and various methyl derivates, unlike cellulose. The role of hemicelluloses as cell wall carbohydrates in hemp structure is to bind strongly to cellulose microfibrils by hydrogen bonds. This polymer dominates in the middle lamella, whereas cellulose is more plentiful in the secondary layers.

Unlike cellulose and hemicelluloses, the chemical structure of lignin cannot be accurately defined. Lignin (21%) is a cross-linked phenolic polymer rich in aromatic substances. The major building blocks are monolignols incorporated into lignin macromolecule as p-hydroxyphenyl, syringyl, and guacyl [28]. Lignin macromolecular structure has a key role in binding cellulose and hemicelluloses together, giving hemp its stiffness.

Pectin is a structural acidic heteropolysaccharide consisting of long-chain galacturonan segments and other neutral sugars such as rhamnose, arabinose, galactose, and xylose. It forms a matrix with celluloses and hemicelluloses, provides structural integrity, strength, and flexibility to the cell wall, and acts as a barrier to the external environment [29].

Cellulose is a crystalline substance, while the other two main constituents of hemp, hemicellulose and lignin, have an amorphous structure. The cellulose crystallinity is a determining parameter of bio-based composites. On the other side, it is important to study the long-term matrix impact on bio-aggregates components.

3.2. FTIR Spectra of Hemp Hurds Samples

Attenuated Total Reflectance Fourier Transform Infrared Spectroscopy as a non-destructive, fast, and convenient vibration technique, useful for providing information on structural changes of molecules in terms of their functional groups of polysaccharides and other organic compounds at the cell wall level [30] was used for the detection of changes in hemp hurds during treatment processing as well as for the identifying surface changes of bio-aggregates incorporated in the composite. The changes in IR spectra due to incorporation of the reference sample, chemically and physicochemically treated hemp hurds in the composite are shown in Figs 1-5. By comparing the spectra of the hemp aggregate samples, taken over the range of 4,000–400 cm^{-1}, we can state that despite the complex chemical composition of the studied samples, the spectra were the consequences of vibrational transitions within dominant hemp hurds constituents and binder components. The FTIR spectra of all hemp hurds samples reveal several major intensive bands that can be divided into the following three significant regions of wave numbers: 3,600-3,000 cm^{-1}, 3,000-2,800 cm^{-1}, and 1,800-700 cm^{-1}. The literature data of characteristic IR vibrations of common functional groups in vegetable fibers were used for assigning bands observed in measured spectra [31].

Due to the complex hemp structure and different construction of the organic polymeric components, the observed spectral bands are discussed separately for each component of the hemp hurds bio-aggregate.

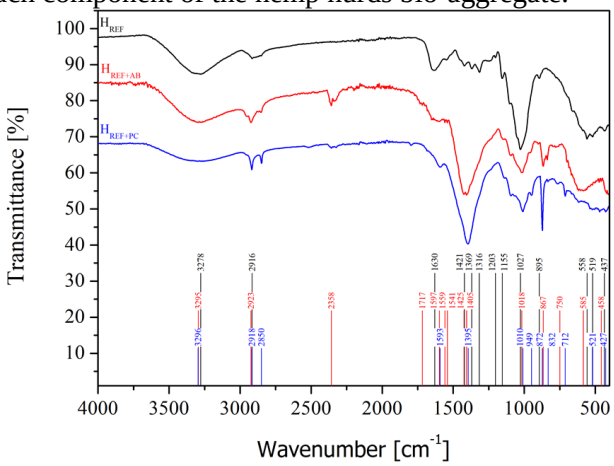

Fig. 1 FTIR spectra of reference hemp hurds (HREF) and long-term embedded in composite based on alternative binder (HREF+AB) and Portland cement (HREF+PC)

3.2.1. Cellulose and Hemicelluloses

A strong, broad peak in the range of 3,490-3,170 cm-^{1} characteristic for stretching vibration of -OH and -CH bonds in polysaccharides is present in the spectra of all samples. This broadband in the spectra range of 3,490-3,170 cm^{-1} represents the complex vibrations of hydroxyl stretching of inter-and intra-molecular hydrogen bonds. Two intermolecular hydrogen bond vibrations in cellulose following [32, 33] appear at 3,319-3,329 cm^{-1} only in chemically and physicochemically modified samples. Peaks observed in the reference sample spectra of hemp hurds, originating from the composite at 3,279-3,298 cm^{-1},

were attributed to the intermolecular hydrogen bonds in triclinic and monoclinic cellulose (I_α and I_β) [34]. The strong broad of –OH stretching in the range mentioned above is also caused by adsorbed moisture.

Another two bands in the regions around 2,945-2,912 cm^{-1} and at about 2,850 cm^{-1} assigned to asymmetric and symmetric stretching modes of aliphatic C-H bonds in the form of methyl and methylene groups are visible in the spectra of all samples [35]. These bands at 2,920, 2912, and 2,849 cm^{-1} are most visible in the hemp hurds modified in $Ca(OH)_2$ and EDTA spectra. A broad peak observed in this region of FTIR spectrum for the reference sample (Fig. 1) probably comprises the CH stretching and bending vibrations of CH_2 and CH_3 in polysaccharides. The CO stretching at 2,900 cm^{-1} and the peak characteristic for waxes and oils at around 2,850 cm^{-1} present in all samples except hemp hurds sample ultrasound treated in NaOH solution (Fig. 5).

As shown in Fig. 2, the intensity of this peak is lower for NaOH treated sample than a reference sample. In the wave numbers range of 1,800 to 900 cm^{-1} with many absorption bands corresponding to the vibration of various functional groups present in hemp components, only the most visible differences in the spectra are presented and discussed.

The typical band demonstrates the presence of hemicelluloses in hemp hurds samples at 1,733 cm^{-1} attributed to the stretching vibration of an unconjugated C=O group in the acetyl groups [32]. This peak was only observed in spectra of reference hemp hurds (Fig. 1) and ultrasound-treated samples (Fig. 5). Chemical attack of alkaline solutions (NaOH and $Ca(OH)_2$) degrades hemicelluloses contained in hemp hurds. As shown in [23], the bio-aggregate surface is roughened after NaOH and $Ca(OH)_2$ treatment.

In the spectra of all samples, the absorption bands observed at 1,155 cm^{-1} correspond to oxygen stretching vibration in C-O-C bonds present in β-glycosidic linkages in hemicellulose and cellulose. The band at 1,103 cm^{-1} belongs to stretching vibrations of C-O and C-C bonds in both components of holocellulose. The peak in the range of 1,032-1,019 cm^{-1} is attributed to C-C, C-OH, C-H ring, and side group vibrations in hemicelluloses.

Typical bands assigned to cellulose were observed at 896 cm^{-1} and in the region of 1,630-1,160 cm^{-1} (Figs 1-5). The absorption band at 896 cm^{-1} is assigned as C-O-C stretching vibration of glycosidic bonds in polysaccharides. The absorption bands assigned to cellulose are observed in all spectra at 1,424 and 1,373 cm^{-1} (-CH_2- and -CH bending vibrations), 1,337 and 896 cm^{-1} (O-H bending vibrations), 1,333-1,316 cm^{-1} (-CH_2- wagging vibration) [36]. In accordance with data in [48], wave numbers at 1,630, 1,369, 1,060 and 896 cm^{-1} are attributed to functional groups in native cellulose.

A significant effect of the alkaline treatment (Fig. 2) and ultrasound modification in NaOH solution (Fig. 5) on the intensity of peak at 1,630 cm^{-1} corresponding to water absorbed in cellulose was observed. According to [37], NaOH reacts with hydroxyl groups present in cellulose, forming the water molecules. Peak around 1,370 cm^{-1} corresponds to CH bending vibration in C-CH_3. The band observed at 1,155 cm^{-1} belongs to C-O-C asymmetric bridge oxygen stretching in amorphous cellulose (cell walls) [38]. In the wave number about 1,150 cm^{-1}, ring vibrations (C-OH) can be overlapped with stretching vibrations of side groups and glycosidic bond vibrations (C-O-C) (hemicelluloses) [39].

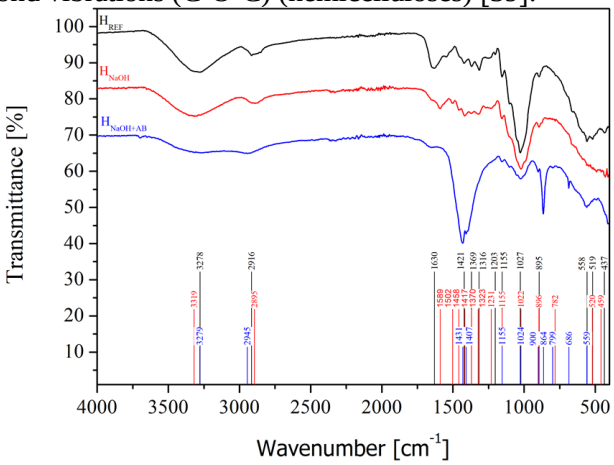

Fig. 2 FTIR spectra of NaOH treated hemp hurds (H_{NaOH}) and long-term embedded in composite based on alternative binder (HNaOH + AB) in comparison to reference hemp hurds (HREF)

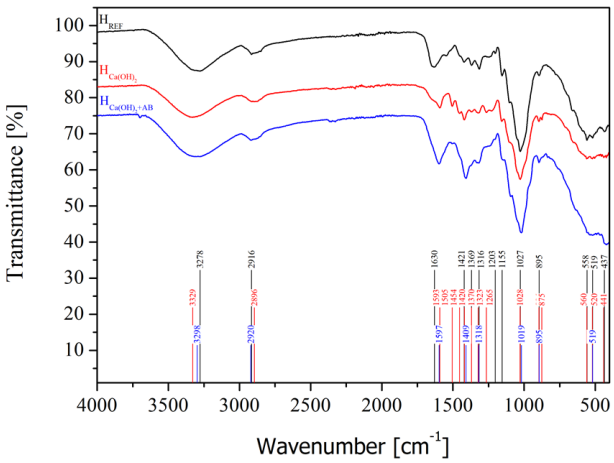

Fig. 3 FTIR spectra of Ca(OH)2 treated hemp hurds (HCa(OH)2) and after its application in composite based on alternative binder (HCa(OH)2 + AB) compared to reference hemp hurds (HREF)

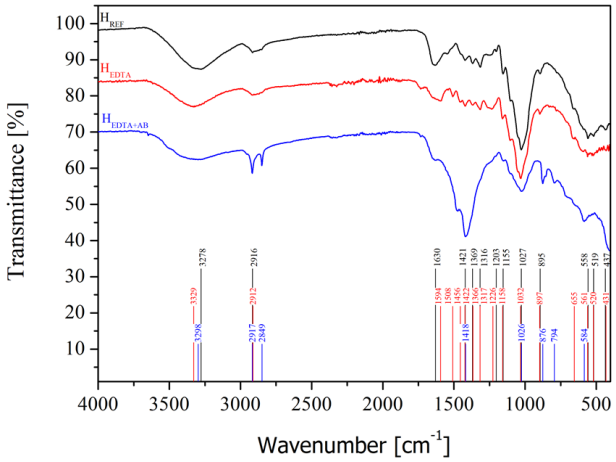

Fig. 4 FTIR spectra of EDTA treated hemp hurds (HEDTA) and long-term embedded in composite based on alternative binder (HEDTA + AB) in comparison to reference hemp hurds (HREF)

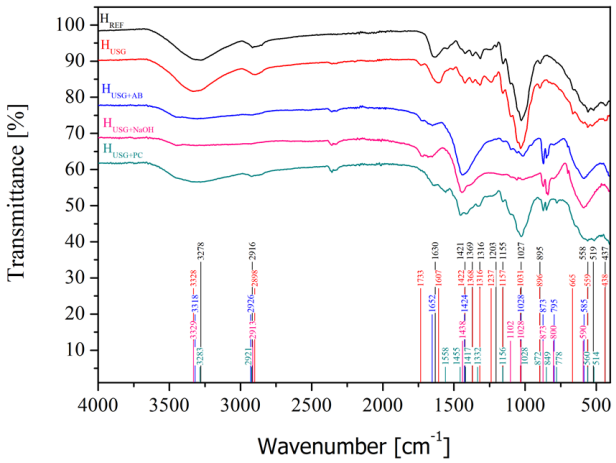

Fig. 4 FTIR spectra of ultrasound treated hemp hurds in water (HUSG) and in NaOH (HUSG + NaOH), long-term embedded samples in composite based on alternative binder (HUSG + AB) and Portland cement (HUSG + PC) in comparison to reference hemp hurds (HREF)

3.2.2. Lignin

Unsuccessful removing lignin from hemp fiber bundles in hurds was indicated by the presence of the sharp peaks located at 1,597-1,589 (aromatic ring vibrations and C=O stretching vibrations) and 1,508 – 1,502 cm^{-1} (C-C stretching from the aromatic ring) in FTIR spectra of $Ca(OH)_2$ and EDTA treated hemp hurds samples. However, NaOH treatment led to partial removal of lignin. This fact confirms the complicated process of lignin degradation or fragmentation due to strong C-C linkages and other very resistant function groups such as aromatic groups [40]. As is evident from Figs 1-5, the other peaks typical for lignin were observed around 1,420 cm^{-1} and 1,320 cm^{-1} in all samples. Lignin is a complex polymer of aromatic alcohols that shows the bands typical for bond vibrations in guaiacyl (1,265 and 1,214 cm^{-1}) overlapping in a broad peak at about 1,230 cm^{-1} and in syringyl (1,320 cm^{-1}). In addition to these peaks typical of lignin, other bands for vibration of groups present in lignin were observed at wave numbers about 1,454, 1,265, and 1,103 cm^{-1}. Also, in-plane and bending aromatic vibrations in syringyl (1,122 cm^{-1}) and guaiacyl units (around 1,027 cm^{-1}) were recorded [41].

3.2.3. Pectin

Analysis of spectra of original hemp hurds sample shows pectin characteristic bands of -OH (around 3,440 cm^{-1}), -CH (around 2,950 cm^{-1}), -COO (1,640 and 1,435 cm^{-1}), -CH (1,240 cm^{-1}), C-O-C (1,145 cm^{-1}) and C-C (1,100 cm^{-1}) vibrations. Absorption of the OH group is also well due to hydrogen bonding of the galacturonic acid in pectin. The -CH stretching and bending vibrations $-CH_2-$ and $-CH_3$ in pectin are included in a broad peak observed in the region of 2,945-2,850 cm^{-1}. Intense peaks in the region 1,000-1,150 cm^{-1} were due to the high homogalacturonan content in pectin [42]. The peak in the range of 1,032-1,019 cm^{-1} belongs to C-C, C-OH, C-H ring, and side group vibrations in pectin. From Figs 1-5, it is evident some similarity of all spectra, but it is difficult to determine the presence of lignin peaks due to their overlapping with vibrations of other bonds. However, typical lignin peaks are not visible in the spectrum of $Ca(OH)_2$ modified sample (Fig. 3), probably due to its ability to trap calcium. Other treatment methods did not lead to pectin removal from hemp structure.

These facts obtained from FTIR spectra about a partial removal of the main non-cellulosic components (hemicelluloses and lignin) and impurities (waxes) from the surface of hemp hurds slices during treatments were confirmed by chemical analysis of modified bio-aggregates [23, 24]. The treatment effectiveness is determined by the used type of procedure and the chemical nature of the reagent. Alkaline treatment by NaOH solution under operating conditions seems to be the most intense degradation of non-cellulosic components in hemp hurds. The spectrum of the ultrasound-treated sample showed no significant changes in the main band's intensity.

3.2.4. Inorganic Compounds

The presence of M-S-H and C-S-H phases in the spectra of hemp hurds samples excluded from composite matrix based on the alternative binder and Portland cement was also studied. The broadness of the M-S-H band between 600 and 710 cm^{-1} indicates a low degree of structural ordering (Figs 1 and 5). The formation of M-S-H from MgO and SiO_2 is a slow and long-term process dependent on the crystallinity degree of starting oxides. The dissolution of MgO, the precipitation of $Mg(OH)_2$, and its dissolution is the rate-limiting step for the formation of M-S-H. As indicated in literature [43], M-S-H phases contain hydroxyl groups bound directly to the silicon and magnesium. The absorption bands below 800 cm^{-1} (458, 585, and 686 cm^{-1}) in the spectra of hemp hurds samples embedded in composite based on AB matrix

(Figs 1-5) could be assigned to the bond formation between magnesium and oxygen.

Cement-based materials are complex multiphase materials with a dominant phase of calcium silicates hydrates (C-S-H). IR spectra of hemp hurds samples excluded from the cement composite show three bands characteristic for C-S-H located in the range between 1,100 and 900 cm^{-1} (broad), at 794, and 460 cm^{-1} assigned to longitudinal SiO_2 lattice vibration, symmetric Si-O-Si stretching and Si-O-Si bending, respectively (Fig. 1 – H_{REF+PC}; Fig. 5 – H_{USG+PC}).

In both hydrated phases, the intensity of peaks corresponding to M-S-H and C-S-H phases varied due to the calcium/silicon ratio and degree of silicate polymerization [44]. Trapping of calcium ions present in the cement by hemp hurds components leads to reduced formation of $Ca(OH)_2$ and C-S-H nucleation centers. In the spectra, the presence of carbonate ions is also visible around 875 cm^{-1} and 1,418 cm^{-1} (Fig. 1 – H_{REF+AB}; Fig. 2 – $H_{NaOH+PC}$; Fig. 3 – $H_{Ca(OH)2}$ and $H_{Ca(OH)2+PC}$; Fig. 4 – $H_{EDTA+PC}$; Fig. 5 – H_{USG+AB} and H_{USG+PC}) due to carbonation process occurring at composite hardening.

3.3. Changes in the Cellulose Crystallinity in Hurd Samples

Changes in composition and structure of the surface of modified lignocellulosic particles strongly influenced the mechanical properties of bio-aggregate-reinforced composites, as shown in [22]. Therefore, the long-termed incorporation behavior of suitably treated hemp hurds in the mineral matrix should be investigated to predict some undesired interactions affecting the durability of bio-aggregates and composite.

Based on published knowledge [23], the treatment process changes cellulose crystalline structures by disrupting cellulose chains' inter- and intra- hydrogen bonding. Also, hydrogen bonding and/or hydroxyl bridges between hydroxyl groups of mineral paste and those in cellulose and lignin are essential for hardening [19]. In order to evaluate the changes in infrared crystallinity of cellulose as the main constituent of hemp hurds, two ratios of IR bands intensities were selected for quantitative analysis as described in part 2.4. The calculated TCI and LOI values of cellulose in hemp hurds samples are given in Table 2 for the ratio of band intensities equal to 1375/2900 and 1423/897. TCI and LOI values were influenced by the treatment process of hemp hurds and their long-term embedding in the composite. According to the literature [45], this increase in cellulose crystallinity during NaOH treatment of hemp hurds can be connected with a loss of the less ordered cellulose. The ratio of TCI and LOI values of NaOH modified sample and reference hemp hurds shows an almost 30% and 40% increase in cellulose crystallinity and ordering.

Table 2 Calculated TCI and LOI in hemp hurds samples

Sample	Hemp Hurds Sample	TCI	LOI
1	Reference (original)	0.93	1.09
2	Reference (original) from AB matrix	0.87	0.94
3	Reference (original) from PC matrix	0.70	0.92
4	NaOH treated	1.20	2.11
5	NaOH treated from AB matrix	0.78	0.82
6	$Ca(OH)_2$ treated	0.96	1.05
7	$Ca(OH)_2$ treated from AB matrix	0.89	0.93
8	EDTA treated	0.93	0.98
9	EDTA treated from AB matrix	0.79	0.78
10	Ultrasound treated in water	0.98	1.14
11	Ultrasound treated in NaOH	0.84	0.89
12	Ultrasound treated from AB matrix	0.77	0.87
13	Ultrasound treated from PC matrix	0.86	0.98

This phenomenon could be attributed to the better ordering of cellulose units due to the destruction of cellulose macromolecular chains during their partial alkaline hydrolysis (NaOH treatment) and pulping the bundles (ultrasound treatment), leading to a decrease in the degree of polymerization [22]. The observed increase in the crystalline fraction of cellulose in hemp hurds agrees with data found for the wood and hemp samples after their alkaline treatment reported in [46, 47]. The increase in crystallinity of cellulose after alkaline treatment of hemp hurds was confirmed by methods of FTIR spectroscopy and XRD analysis. However, other values of the crystallinity index have been found [23].

Ultrasound treatment in water shows slightly higher TCI and LOI values than the reference sample. On the other hand, the TCI and LOI values for other treated samples ($Ca(OH)_2$ and EDTA) were close to those for the reference sample. The combined NaOH and ultrasound treatment of hemp hurds led to a slightly lower crystallinity value indicating a more disordered cellulose structure than the reference sample. Differences in the TCI and LOI values of these modified samples can also be caused by the inhomogeneity of the samples, which was reflected in the measurement of the intensities of the corresponding peaks.

As shown in Table 2, the cellulose crystallinity of hemp hurds (TCI and LOI values) is affected not only by structural and compositional changes due to the treatment process but also by alkaline binder nature and interaction bio-aggregates with binder particles during their long-term embedding in the composite.

Based on comparing the TCI and LOI values of MgO-cement matrix embedded samples, no impact of this binder on $Ca(OH)_2$ treated sample was appeared due to forming a protective layer on the surface of aggregates. In contrast, cellulose crystallinity of other hemp hurds samples was lower than those of the reference sample originating from composite with AB matrix. These results are probably related to continuing

destruction of cellulose macromolecular chains during their partial hydrolysis in alkaline medium of MgO-cement.

Other behavior of hemp hurds samples (reference and ultrasound modified) after its long-term incorporation in Portland cement composite was found. For ultrasound treated bio-aggregate reinforcing the composite of higher compressive strength than composite based on original hemp [40], the obtained TCI and LOI values were more favorable (0.86; 0.98) than those of comparing original hemp hurds sample (0.70; 0.92). As known, the alkaline environment of MgO-cement is represented by a higher pH value due to the presence of $NaHCO_3$ component in the alternative binder in comparison to the pH of Portland cement paste [48]. Therefore the explanation of this finding is related to a less impact of the alkaline medium of Portland cement on cellulose [49].

4. Conclusion

In this study, FTIR analyses have been carried out to characterize changes resulting from the long-term interaction between untreated and treated hemp hurds and alternative binder matrix of MgO-cement. To this purpose, six-year-old composite embedded plant waste bio-aggregate and its chemically and physicochemically surface-modified products have been used. To help identify changes in the behavior of hemp hurds embedded in the MgO-cement matrix, bio-aggregate samples from Portland cement composite were also used. Particular attention has been given to this long-term interaction; no data is reported in the scientific literature. The first part of the results obtained from the detailed spectrum analysis of all modified hemp hurds samples confirmed a partial degradation of hemp hurds constituents induced by different treatments. Based on the presented results, it can be suggested that only the NaOH treatment was effective in removing hemicellulose and lignin. The treatment performance of bio-aggregate samples has also been evaluated by cellulose crystallinity. The content of the crystalline phase of cellulose was affected by the extent of degradation. The higher TCI and LOI values observed after alkaline treatment by NaOH compared to untreated hemp hurds indicated an increase in crystallinity and a more ordered cellulose structure. This increase in cellulose crystallinity can be attributed to the reduction of amorphous fractions in the complex structure of hemp hurds.

Cellulose crystallinity of hemp hurds (TCI and LOI values) is influenced not only by structural and compositional changes due to the treatment process but also by interaction with binder particles during long-term embedding of bio-aggregates in the composite mineral matrix of MgO-cement and Portland cement. The evaluation of bio-aggregate samples' performance due to their long-term incorporation in composite matrix confirmed an effect of the alkaline environment of binders on cellulose crystallinity. Due to the lower alkalinity of Portland cement paste, a higher degree of cellulose crystallinity in the studied embedded hemp hurds samples was found.

These results underline the need to investigate further specific treatments of hemp hurds in response to their behaviors exhibited by the binder matrix. Future research is planned using other more sensitive analytical techniques such as ATR-FTIR microscopic mapping and imaging, X-ray photoelectron spectroscopy (XPS), and nuclear magnetic resonance (NMR) to characterize both organic and inorganic constituents present on the surface of embedded bio-aggregate in lower portions.

Acknowledgments

The authors are grateful to the Agency of the Ministry of the Education, Science, Research, and Sport of the Slovak Republic for supporting the project 1/0222/19.

References

[1] PATEL M., PARDHI B., CHOPARA S., and PAL M. Lightweight composite materials for automotive – A review. *International Research Journal of Engineering and Technology*, 2018, 5: 41-47.

[2] RAJAK D.K., PAGAR D.D., KUMAR R., and PRUNCU C.I. Recent progress of reinforcement materials: a comprehensive overview of composite materials. *Journal of Materials Research and Technology*, 2019, 8: 6354-6374. DOI: 10.1016/jrmt.2019.09.068.

[3] FAN M. & FU F. Introduction: A perspective – natural fibre composites in construction. In: FAN M., FU F. (eds.) *Advanced High Strength Natural Fibre Composites in Construction*. Woodhead Publishing Series, Elsevier: Cambridge, United Kingdom, 2017: 1-20.

[4] FAN M. Future scope and intelligence of natural fibre based construction composites. In: FAN M., FU F. (eds.) *Advanced High Strength Natural Fibre Composites in Construction*. Woodhead Publishing Series, Elsevier: Cambridge, United Kingdom, 2017: 545-556.

[5] ZWAWI M. A review on natural fiber bio-composites, surface modifications and applications. *Molecules*, 2021, 26(2): 404. DOI: 10.3.390/molecules26020404.

[6] AMZIANE S. & COLLET F. *Bio-Aggregates Based Building Materials*. State-Of-The-Art Report of the Rilem Technical Committee 236-BBM. Springer: Netherlands, 2017. https://www.springer.com/gp/book/9789402410303.

[7] RUANO G., BELLOMO F., LÓPEZ G., BERTUZZIA A., NALLIMA L., and OLLERB S. Mechanical behaviour of cementitious composites reinforced with bagasse and hemp fibers. *Construction and Building Materials*, 2020, 240: 117856. DOI: 10.1016/j.conbuildmat.2019.117856.

[8] VIEL M., COLLET F., and LANOS C. Chemical and multi-physical characterization of agro-resources' by-product as a possible raw building material. *Industrial Crops and Production*, 2018, 120: 214-237: DOI: 10.1016/j.indcrop.2018.04.025.

[9] AMZIANE S. & SONEBI M. Overview on biobased building material made with plant aggregate. *Rilem Technical Letters*, 2016, 1: 31–38. DOI: 10.21809/rilemtechlett.v1.9.
[10] YASHAS GOWDA T. G., RANGAPPA S. M., PARAMESWARANPILLAI J., and SIENGCHIN S. Natural fibers as sustainable and renewable resource for development of eco-friendly composites: A comprehensive review. *Frontiers in Materials*, 2019, 6: 1-14. DOI: 10.3389/fmats.2019.00226.
[11] BENNICH T. & BELYAZID S. The route to sustainability—prospects and challenges of the bio-based economy. *Sustainability*, 2017, 9: 1-18. DOI: 10.3390/su90608887.
[12] CRINI G., LICHTFOUSE E., CHANET G., and CRINI N. Applications of hemp in textiles, paper industry, insulation and building materials, horticulture, animal nutrition, food and beverages, nutraceuticals, cosmetics and hygiene, medicine, agrochemistry, energy production and environment: a review. *Environmental Chemistry Letters*, 2020, 18(5): 1451-1476. DOI: 10.1007/s10311-018-0812-x.
[13] INGRAM C., LO G.A., BACENETTI J., TRICASE C., DOTELLI G., FIALA M., SIRACUSA V., and MBOHWA C. Energy and environmental assessment of industrial hemp for building applications: A review. *Renewable and Sustainable Energy Reviews*, 2015, 51: 19-42. DOI: 10.1016/j.rser.2015.06.002.
[14] PICKERING K.L, EFENDY M.G.A., and LE T.M. A review of recent developments in natural fibre composites and their mechanical performance. *Composites Part A: Applied Science and Manufacturing*, 2016, 83: 98–112. DOI: 10.1016/compositesa.2015.08.038.
[15] HOLMER S.J., FIORELLI J., and DOS SANTOS S.F. *Sustainable and Nonconventional Construction Materials Using Inorganic Bonded Fiber Composites*. Woodhead Publishing: Duxford, UK, 2017.
[16] DELANNOY G., MARCEAU S., GLÉ P., GOURLAY E., MINERBE M.G., DIAFI D., AMZIANE S., FARCAS F. Impact of hemp shiv extractives on hydration of Portland cement. *Construction and Building Materials*, 2020, 244: 118300. DOI: 10.1016/conbuildmat.2020.118300
[17] DELANNOY G., MARCEAU S., GLÉ P., GOURLAY E., GUÉGUEN-MINERBE M., DIAFI D., NOUR I., AMZIANE S., and FARCAS F. Influence of binder on the multiscale properties of hemp concretes. *European Journal of Environmental and Civil Engineering*, 2019, 23: 609–625. DOI: 10.1080/19648189.2018.1457571.
[18] TANASA F., ZANOAGA M., TEACA C.A., NECHIFOR M., and SHAHZAD A. Modified hemp fibers intended for fiber-reinforced polymer composites used in structural applications—A review. I. Methods of modification. *Polymer Composites*, 2020, 41(1): 5-31. DOI: 10.1002/pc.25354.
[19] MAGNIONT C. & ESCADEILLAS G. Chemical composition of bio-aggregates and their interactions with mineral binders. In: AMZIANE S., COLLET F. (eds.) *Bio-Aggregates Based Building Materials RILEM State-of-the-Art Reports*, 2017: 1–37. DOI: 10.1007/978-94-024-1031-0.
[20] SINKA M., VAN DEN HEEDE P., De BELIE N., BAJAREA D., SAHMENKOA G., and KORJAKINSA A. Comparative life cycle assessment of magnesium binders as an alternative for hemp concrete. *Resources, Conservation and Recycling*, 2018, 133: 288–299. DOI: 10.1016/j.resconrec.2018.02.024.
[21] WANG R., QIN L., and GAO X. Mechanical strength and water resistance of magnesium oxysulfate cement based lightweight materials. *Cement and Concrete Composites*, 2020, 109: 103554. DOI: 10.1016/j.cemconcomp.2020.103554.
[22] STEVULOVA N., CIGASOVA J., SCHWARZOVA I., SICAKOVA A., and JUNAK J. Sustainable bio-aggregate-based composites containing hemp hurds and alternative binder. *Buildings*, 2018, 8(2): 25. DOI: 10.3390/buildings8020025.
[23] STEVULOVA N., CIGASOVA J., ESTOKOVA A., TERPAKOVA E., GEFFERT A., KACIK F., SINGOVSZKA E., and HOLUB M. Properties characterization of chemically modified hemp hurds. *Materials*, 2014, 7: 8131-8150. DOI: 10.3390/ma7128131.
[24] STEVULOVA N., ESTOKOVA A., CIGASOVA J., SCHWARZOVA I., KACIK F., and GEFFERT A. Thermal degradation of natural and treated hemp hurds under air and nitrogen atmosphere. *Journal of Thermal Analysis and Calorimetry*, 2017, 128: 1649–1660. DOI: 10.1007/s10973-016-6044-z.
[25] STEVULOVA N., JUNAK J., and VACLAVIK V.V. Effect of silica fume as a component of alternative binder on the selected technically important characteristics of bio-aggregate-based composites. *Materials*, 2018, 11: 1-9. DOI: 10.3390/ma11112153.
[26] NELSON M.L. & O'CONNOR R.T. Relation of certain infrared bands to cellulose crystallinity and crystal lattice type. Part I. Spectra of lattice types I, II, III and amorphous cellulose. *Journal of Applied Polymer Science*, 1964, 8: 1311–1324. DOI: 10.1002/app.1964.070080323.
[27] MORIN-CRINI N., LOIACONO S., PLACET V., TORRI G., BRADU C., KOSTIĆ M., COSENTINO C., CHANET G., MARTEL B., LICHTFOUSE E., and CRINI G. Hemp-Based Materials for Metal Removal. In: CRINI G., LICHTFOUSE E. (eds.) *Green Adsorbents for Pollutant Removal: Innovative materials*, 2018, 19: 1-34. Springer: Cham. DOI: 10.1007/978-3-319-92162-4_1.
[28] LOURENÇO A. & PEREIRA H. Compositional Variability of Lignin in Biomass. In: POLETTO M. (ed.) *Lignin – Trends and Applications*. IntechOpen: London, United Kingdom, 2018: 65-98. DOI: 10.5772/intechopen.71208.
[29] VANITHA T. and KHAN M. Role of Pectin in Food Processing and Food Packaging. In MASUELLI M. (ed.) *Pectins – Extraction, Purification, Characterization and Applications*. IntechOpen: London, United Kingdom, 2020: 1-22. DOI: 10.5772/intechopen.83677.
[30] LAN W., RENARD C.M.G.C., JAILLAIS B., LECAA A., and BUREAUA S. Fresh, freeze-dried or cell wall samples: Which is the most appropriate to determine chemical, structural and rheological variations during apple processing using ATR-FTIR spectroscopy. *Food Chemistry*, 2020, 330: 127357. DOI: 10.1016/j.foodchem.2020.127357.
[31] CHABANNES M., GARCIA-DIAZ E., CLERC L., and BÉNÉZET J.-C. Effect of curing conditions and Ca(OH)2-treated aggregates on mechanical properties of rice husk and hemp concretes using a lime-based binder. *Construction and Building Materials*, 2016, 102: 821–833. DOI: 10.1016/j.conbuildmat.2015.10.206.

[32] Plymouth University. *Composites Design and Manufacture*. MATS347 MooDLE Student Portal, UK. [Online]. Available from: http://www.fose1.plymouth.ac.uk/smemats347/FTIR_of_natural_fibres.htm.
[33] JAYAMANI E., LOONG T.G., and BIN BAKRI M.K. Comparative study of Fourier transform infrared spectroscopy (FTIR) analysis of natural fibres treated with chemical, physical and biological methods. *Polymers Bulletin*, 2020, 77: 1605–1629. DOI: 10.1007/s00289-019-02824-w.
[34] HISHIKAWA Y., TOGAWA E., and KONDO T. Characterization of individual hydrogen bonds in crystalline regenerated cellulose using resolved polarized FTIR. *American Chemical Society Omega*, 2017, 2(4): 1469–1476. DOI: 10.1021/acsomega.6b00364.
[35] BIN BAKRI M.K. & JAYAMANI E. Comparative study of functional groups in natural fibers: Fourier Transform Infrared Analysis (FTIR). *International Journal of Current Engineering and Scientific Research*, 2016, 3(1): Conference on Futuristic Trends in Engineering, Science, Humanities, and Technology (FTESHT-16), 2016: 154-161.
[36] LIU X., RENARD C.M.G.C., BUREAU S., and LE BOURVELLEC C. Revisiting the contribution of ATR-FTIR spectroscopy to characterize plant cell wall polysaccharides. *Carbohydrate Polymers*, 2021, 262: 117935. DOI: 10.1016/j.carbpol.2021.117935.
[37] YANG Y.P., ZHANG Y., LANG Y.X., and YU M.H. Structural ATR-IR analysis of cellulosic fibers prepared from a NaOH complex aqueous solution. *Materials Science and Engineering*, 2017, 213: 1-7.
[38] CANTERI M.H.G., RENARD C.M.G.C., LE BOURVELLEC C., and BUREAU S. ATR-FTIR spectroscopy to determine cell wall composition: Application on a large diversity of fruits and vegetables. *Carbohydrate Polymers*, 2019, 212: 186-196. DOI: 10.1016/j.carbpol.2019.02.021.
[39] SZSYMANSKA-CHARGOT M., CHYLINSKA M., KRUK B., and ZDUNEK A. Combining FT-IR spectroscopy and multivariate analysis for qualitative and quantitative analysis of the cell wall composition changes during apples development. *Carbohydrate Polymers*, 2015, 115: 93-103. DOI: 10.1016/j.carbpol.2014.08.039.
[40] PEJIĆ B.M., KRAMAR A.D., OBRADOVIĆ B.M., MILORAD M.K., ŽEKIĆB A.A., and KOSTIĆA M.M. Effect of plasma treatment on chemical composition, structure and sorption properties of lignocellulosic hemp fibers (Cannabis sativa L.). *Carbohydrate Polymers*, 2020, 236: 116000. DOI: 10.1016/j.carbpol.2020.116000.
[41] DE FRANÇA S.J., DE SOUSA S.J., BORGES C.L.R., MICOLIB L., SILVA L.M.A., CANUTO K.M., DE MACEDOA A.C., and ROCHAA M.V.P. Extraction and characterization of lignins from cashew apple bagasse obtained by different treatments. *Biomass and Bioenergy*, 2020, 141: 105728. DOI: 10.1016/j.biombioe.2020.105728.
[42] SANTOS E.E., AMARO R.C., BUSTAMANTE C.C.C., GUERRA M.H.A., CATONE S.L., and FROES R.E.S. Extraction of pectin from agroindustrial residue with an eco-friendly solvent: use of FTIR and chemometrics to differentiate pectins according to degree of methyl esterification. *Food Hydrocolloids*, 2020, 107: 105921. DOI: 10.1016/j.foodhyd.2020.105921.
[43] NIED D., ENEMARK-RASMUSSEN K., L'HOPITAL E., SKIBSTED J., and LOTHENBACH B. Properties of magnesium silicate hydrates (MSH). *Cement and Concrete Research*, 2016, 79: 323-332. DOI: 10.1016/j.cemconres.2015.10.003.
[44] KUNTHER W., FERREIRO S., and SKIBSTED J. Influence of the Ca/Si ratio on the compressive strength of cementitious calcium-silicate-hydrate binders. *Journal of Material Chemistry A*, 2017, 5: 17401-17412. DOI: 10.1039/c7ta06104h.
[45] CARRIÓN-PRIETO C., MARTIN-RAMOS P., HERNÁNDEZ-NAVARRO S., SÁNCHEZ-SASTRE L.F., MARCOS-ROBLES J.L., and MARTÍN-GIL J. Crystallinity of cellulose microfibers derived from Cistus Ladaifer and Erica Arborea Shrubs. *Maderas-Ciencia y Tecnologia*, 2019, 21: 447-456. DOI: 10.4067/S0718-221X2019005000402.
[46] LIONETTO F., DEL SOLE R., CANNOLETTA D., VASAPOLLO G., and MAFFEZZOLI A. Monitoring wood degradation during weathering by cellulose crystallinity. *Materials*, 2012, 5: 1910-1922. DOI: 10.3390/ma5101910.
[47] VISCUSI G., BARRA G., and GORRASI G. Modification of hemp fibers through alkaline attack assisted by mechanical milling: effect of processing time on the morphology of the system. *Cellulose*, 2020, 27: 8653-8665. DOI: 10.1007/s10570-020-03406-0.
[48] STEVULOVA N, SCHWARZOVA I., ESTOKOVA A., and HOLUB M. MgO-based cement as an inorganic binder for hemp hurds composites. *Cheminé Technologija*, 2016, 67: 24-29. DOI: 10.5755/j.ct.67.1.15000.
[49] DIQUELOU Y., GOURLAY E., ARNAUD L., and KUREK B. Impact of hemp shive on cement setting and hardening: Influence of the extracted components from the aggregates and study of the interfaces with the inorganic matrix. *Cement and Concrete Composites*, 2015, 55: 112-121. DOI: 10.1016/j.cemconcomp.2014.09.004.

参考文:

[1] PATEL M.、PARDHI B.、CHOPARA S. 和 PAL M. 汽車輕量化複合材料—綜述。國際工程技術研究雜誌，2018，5：41-47。
[2] RAJAK D.K.、PAGAR D.D.、KUMAR R. 和 PRUNCU C.I. 增強材料的最新進展：複合材料綜合綜述.材料研究與技術雜誌，2019，8：6354-6374。DOI：10.1016/jrmt.2019.09.068。
[3] FAN M. 和 FU F. 介紹：觀點—建築中的天然纖維複合材料。見：FAN M., FU F. (編輯。) 建築中的高級高強度天然纖維複合材料。伍德黑德出版系列，愛思唯爾：英國劍橋，2017：1-20。
[4] FAN M. 天然纖維基建築複合材料的未來範圍和智能。見：FAN M., FU F. (編輯。) 建築中的高級高強度天然纖維複合材料。伍德黑德出版系列，愛思唯爾：英國劍橋，2017：545-556。
[5] ZWAWI M. 天然纖維生物複合材料、表面改性和應用綜述。分子，2021，26(2)：404。DOI：10.3.390/molecules26020404。

[6] AMZIANE S. 和 COLLET F. 基於生物聚集體的建築材料。寬慰技術委員會的最新報告。斯普林格：荷蘭，2017 年。https://www.springer.com/gp/book/9789402410303。

[7] RUANO G.、BELLOMO F.、LÓPEZ G.、BERTUZZIA A.、NALLIMA L. 和 OLLERB S. 用甘蔗渣和大麻纖維增強的水泥基複合材料的機械性能。建築與建築材料，2020，240：117856。DOI：10.1016/j.conbuildmat.2019.117856。

[8] VIEL M.、COLLET F. 和 LANOS C. 作為可能的建築原材料的農業資源副產品的化學和多物理特性。工業作物和生產，2018 年，120：214-237：DOI：10.1016/j.indcrop.2018.04.025。

[9] AMZIANE S. 和 SONEBI M. 植物骨料製成的生物基建築材料概述。寬慰技術快報，2016 年，1：31-38。 DOI：10.21809/rilemtechlett.v1.9。

[10] YASHAS GOWDA T. G.、RANGAPPA S. M.、PARAMESWARANPILLAI J. 和 SIENGCHIN S. 天然纖維作為可持續和可再生資源用於開發環保複合材料：綜合評論。材料前沿， 2019， 6: 1-14。 DOI：10.3389/fmats.2019.00226。

[11] BENNICH T. 和 BELYAZID S. 可持續發展之路—生物基經濟的前景和挑戰。可持續性， 2017， 9: 1-18。 DOI：10.3390/su90608887。

[12] CRINI G.、LICHTFOUSE E.、CHANET G. 和 CRINI N. 大麻在紡織品、造紙工業、絕緣和建築材料、園藝、動物營養、食品和飲料、營養保健品、化妝品和衛生、醫藥中的應用，農業化學、能源生產和環境：綜述。環境化學快報， 2020， 18(5): 1451-1476。 DOI：10.1007/s10311-018-0812-x。

[13] INGRAM C.、LO G.A.、BACENETTI J.、TRICASE C.、DOTELLI G.、FIALA M.、SIRACUSA V. 和 MBOHWA C. 建築應用工業大麻的能源和環境評估：綜述。可再生和可持續能源評論，2015 年，51：19-42。 DOI：10.1016/j.rser.2015.06.002。

[14] 皮克林 K.L、EFENDY M.G.A. 和 LE T.M. 天然纖維複合材料及其機械性能的最新發展綜述。複合材料一种部分：應用科學與製造，2016 年，83：98-112。 DOI：10.1016/compositesa.2015.08.038。

[15] HOLMER S.J.、FIORELLI J. 和 DOS SANTOS S.F.使用無機粘合纖維複合材料的可持續和非常規建築材料。伍德黑德出版社：英國達克斯福德，2017 年。

[16] DELANNOY G.、MARCEAU S.、GLÉ P.、GOURLAY E.、MINERBE M.G.、DIAFI D.、AMZIANE S.、FARCAS F. 大麻提取物對波特蘭水泥水化的影響。建築與建材，2020，244：118300。DOI：10.1016/conbuildmat.2020.118300

[17] DELANNOY G.、MARCEAU S.、GLÉ P.、GOURLAY E.、GUÉGUEN-MINERBE M.、DIAFI D.、NOUR I.、AMZIANE S. 和 FARCAS F. 粘合劑對大麻多尺度特性的影響混凝土。歐洲環境與土木工程雜誌，2019 年，23：609-625。DOI：10.1080/19648189.2018.1457571。

[18] TANASA F.、ZANOAGA M.、TEACA C.A.、NECHIFOR M. 和 SHAHZAD A. 用於結構應用中使用的纖維增強聚合物複合材料的改性大麻纖維═綜述。一、修改方法。聚合物複合材料，2020, 41(1): 5-31。 DOI：10.1002/pc.25354。

[19] MAGNIONT C. 和 ESCADEILLAS G. 生物聚集體的化學成分及其與礦物粘合劑的相互作用。在：AMZIANE S., COLLET F. (編輯。) 基於生物聚集體的建築材料寬慰最新報告，2017：1-37。 DOI：10.1007/978-94-024-1031-0。

[20] SINKA M.、VAN DEN HEEDE P.、De BELIE N.、BAJAREA D.、SAHMENKOA G. 和 KORJAKINSA A. 鎂粘合劑作為大麻混凝土替代品的生命週期比較評估。資源、保護和回收，2018 年，133：288-299。DOI：10.1016/j.resconrec.2018.02.024。

[21] WANG R., QIN L., 和GAO X. 硫酸鎂水泥基輕質材料的機械強度和耐水性。水泥和混凝土複合材料，2020，109：103554。DOI：10.1016/j.cemconcomp.2020.103554。

[22] STEVULOVA N.、CIGASOVA J.、SCHWARZOVA I.、SICAKOVA A. 和 JUNAK J. 含有大麻纖維和替代粘合劑的可持續生物聚集基複合材料。建築物，2018 年，8(2)：25。DOI：10.3390/buildings8020025。

[23] STEVULOVA N.、CIGASOVA J.、ESTOKOVA A.、TERPAKOVA E.、GEFFERT A.、KACIK F.、SINGOVSZKA E. 和 HOLUB M. 化學改性大麻 障礙的特性表徵。材料，2014，7：8131-8150。 DOI：10.3390/ma7128131。

[24] STEVULOVA N.、ESTOKOVA A.、CIGASOVA J.、SCHWARZOVA I.、KACIK F. 和 GEFFERT A. 在空氣和氮氣氣氛下天然和處理過的大麻纖維的熱降解。熱分析和量熱雜誌，2017，128：1649-1660。 DOI：10.1007/s10973-016-6044-z。

[25] STEVULOVA N.、JUNAK J. 和 VACLAVIK V.V. 矽粉作為替代粘合劑的成分對生物集料基複合材料選定的技術重要特性的影響。材料，2018，11：1-9。 DOI：10.3390/ma11112153。

[26] NELSON M.L. 和O'CONNOR R.T. 某些紅外波段與纖維素結晶度和晶格類型的關係。第 I 部分。 I、II、III 型晶格和無定形纖維素的光譜。應用高分子科學雜誌，1964，8：1311-1324。DOI：10.1002/app.1964.070080323。

[27] MORIN-CRINI N.、LOIACONO S.、PLACET V.、TORRI G.、BRADU C.、KOSTIĆ M.、COSENTINO C.、CHANET G.、MARTEL B.、LICHTFOUSE E. 和 CRINI G. 麻-用於去除金屬的材料。見：CRINI G., LICHTFOUSE E. (編輯。) 去除污染物的綠色吸附劑：創新材料，2018 年，19：1-34。斯普林格：查姆。 DOI：10.1007/978-3-319-92162-4_1。

[28] LOURENÇO A. 和 PEREIRA H. 生物質中木質素的成分變異性。在：POLETTO M. (和。) 木質素—

趨勢和應用。英泰開放：英國倫敦，2018：65-98。DOI：10.5772/intechopen.71208。
[29] VANITHA T. 和 KHAN M. 果膠在食品加工和食品包裝中的作用。在 MASUELLI M. (和。) 果膠 - 提取、純化、表徵和應用中。英泰開放：英國倫敦，2020 年：1-22。 DOI：10.5772/intechopen.83677。
[30] LAN W.、RENARD CMGC、JAILLAIS B.、LECAA A. 和 BUREAUA S. 新鮮、冷凍乾燥或細胞壁樣品：哪種最適合使用衰減全反射
確定蘋果加工過程中的化學、結構和流變學變化-紅外光譜光譜。食品化學，2020，330：127357。DOI：10.1016/j.foodchem.2020.127357。
[31] CHABANNES M.、GARCIA-DIAZ E.、CLERC L. 和 BÉNÉZET J.-C. 養護條件和氫氧化鈣處理的骨料對使用石灰基粘合劑的稻殼和大麻混凝土力學性能的影響。建築和建築材料，2016，102：821-833。DOI：10.1016/j.conbuildmat.2015.10.206。
[32] 普利茅斯大學。複合材料設計和製造。地墊347模版學生門戶，英國。[在線的]。可從：http://www.fose1.plymouth.ac.uk/smemats347/FTIR_of_natural_fibers.htm 獲得。
[33] JAYAMANI E.、LOONG T.G. 和 BIN BAKRI M.K.用化學、物理和生物方法處理的天然纖維的傅里葉變換紅外光譜 (紅外光譜) 分析的比較研究。聚合物公報，2020 年，77：1605-1629。DOI：10.1007/s00289-019-02824-w。
[34] HISHIKAWA Y.、TOGAWA E. 和 KONDO T. 使用分辨偏振 紅外光譜表徵結晶再生纖維素中的單個氫鍵。美國化學學會歐米茄, 2017, 2(4): 1469‑1476。DOI：10.1021/acsomega.6b00364。
[35] BIN BAKRI M.K. 和 JAYAMANI E. 天然纖維中官能團的比較研究：傅里葉變換紅外分析 (紅外光譜)。國際當代工程與科學研究雜誌，2016，3(1): 工程、科學、人文和技術未來趨勢會議, 2016: 154-161。
[36] LIU X.、RENARD C.M.G.C.、BUREAU S.、和LE BOURVELLEC C. 重新審視 衰減全反射-紅外光譜光譜對錶徵植物細胞壁多醣的貢獻。碳水化合物聚合物，2021，262：117935。DOI：10.1016/j.carbpol.2021.117935。
[37] YANG Y.P., ZHANG Y., LAN Y.X., 和YU M.H. 由氫氧化鈉複合物水溶液製備的纖維素纖維的結構衰減全反射-IR 分析。材料科學與工程，2017，213：1-7。
[38] CANTERI M.H.G.、RENARD C.M.G.C.、LE BOURVELLEC C. 和 BUREAU S. 衰減全反射-紅外光譜光譜法測定細胞壁組成：在多種水果和蔬菜上的應用。碳水化合物聚合物，2019，212：186-196。DOI：10.1016/j.carbpol.2019.02.021。
[39] SZSYMANSKA-CHARGOT M.、CHYLINSKA M.、KRUK B. 和 ZDUNEK A. 結合紅外光譜光譜和多變量分析對蘋果發育過程中細胞壁成分變化的定性和定量分析。碳水化合物聚合物, 2015, 115: 93-103。DOI：10.1016/j.carbpol.2014.08.039。
[40] PEJIĆ B.M.、KRAMAR A.D.、OBRADOVIĆ B.M.、MILORAD M.K.、ŽEKIĆB A.A. 和 KOSTIĆA M.M. 等離子體處理對木質纖維素大麻纖維 (大麻 L.) 的化學成分、結構和吸附性能的影響。碳水化合物聚合物，2020 年，236：116000。DOI：10.1016/j.carbpol.2020.116000。
[41] DE FRANÇA S.J.、DE SOUSA S.J.、BORGES C.L.R.、MICOLIB L.、SILVA L.M.A.、CANUTO K.M.、DE MACEDOA A.C. 和 ROCHAA M.V.P. 不同處理所得腰果蘋果蔗渣木質素的提取與表徵.生物質與生物能源，2020，141：105728。DOI：10.1016/j.biombioe.2020.105728。
[42] SANTOS E.E.、AMARO R.C.、BUSTAMANTE C.C.C.、GUERRA M.H.A.、CATONE S.L. 和 FROES R.E.S. 使用環保溶劑從農業工業殘留物中提取果膠：使用紅外光譜
和化學計量學根據甲酯化程度區分果膠。食品親水膠體，2020，107：105921。DOI：10.1016/j.foodhyd.2020.105921。
[43] NIED D.、ENEMARK-RASMUSSEN K.、L'HOPITAL E.、SKIBSTED J. 和 LOTHENBACH B. 矽酸鎂水合物的特性。水泥和混凝土研究，2016，79：323-332。 DOI：10.1016/j.cemconres.2015.10.003。
[44] KUNTHER W.、FERREIRO S. 和 SKIBSTED J. 作為比對水化矽酸鈣粘結劑抗壓強度的影響。材料化學雜誌一種, 2017, 5: 17401-17412。DOI：10.1039/c7ta06104h。
[45] CARRIÓN-PRIETO C., MARTIN-RAMOS P., HERNÁNDEZ-NAVARRO S., SÁNCHEZ-SASTRE L.F., MARCOS-ROBLES J.L., 和 MARTÍN-GIL J. 源自岩薔薇和埃麗卡的纖維素微纖維的結晶度。木材科技, 2019, 21: 447-456。DOI：10.4067/S0718-221X2019005000402。
[46] LIONETTO F.、DEL SOLE R.、CANNOLETTA D.、VASAPOLLO G. 和 MAFFEZZOLI A. 通過纖維素結晶度監測風化過程中的木材降解。材料，2012，5：1910-1922。 DOI：10.3390/ma5101910。
[47] VISCUSI G.、BARRA G. 和 GORRASI G. 通過機械研磨輔助的鹼侵蝕對大麻纖維的改性：處理時間對系統形態的影響。纖維素，2020，27：8653-8665。DOI：10.1007/s10570-020-03406-0。
[48] STEVULOVA N、SCHWARZOVA I.、ESTOKOVA A. 和 HOLUB M. 氧化鎂基水泥作為大麻 障礙複合材料的無機粘合劑。化學技術，2016，67：24-29。DOI：10.5755/j.ct.67.1.15000。
[49] DIQUELOU Y.、GOURLAY E.、ARNAUD L. 和 KUREK B. 大麻碎屑對水泥凝固和硬化的影響：從骨料中提取成分的影響以及與無機基質界面的研究。水泥和混凝土複合材料，2015 年，55：112-121。DOI：10.1016/j.cemconcomp.2014.09.004。